Optics Communications 312 (2014) 163–167

Contents lists available at ScienceDirect

Optics Communications

journal homepage: www.elsevier.com/locate/optcom

Passively Q-switched microchip lasers based on Yb:YAG/Cr^{4+}:YAG composite crystal

Yingying Ren, Jun Dong *

Department of Electronic Engineering, School of Information Science and Technology, Xiamen University, Xiamen 361005, China

ARTICLE INFO

Article history:
Received 21 May 2013
Received in revised form
11 September 2013
Accepted 14 September 2013
Available online 24 September 2013

Keywords:
Composite crystal
Microchip lasers
Passively Q-switched
Yb:YAG
Cr^{4+}:YAG
Laser-diode pumping

ABSTRACT

Efficient passively Q-switched microchip laser based on Yb:YAG/Cr^{4+}:YAG composite crystal has been demonstrated under high brightness single-emitter laser-diode pumping. Maximum average output power of 1.5 W was obtained when the absorbed pump power was 3.65 W, the corresponding optical-to-optical efficiency was over 41%. The slope efficiency was 52.3%. The effect of the cavity length on the performance of Yb:YAG/Cr^{4+}:YAG composite crystal passively Q-switched microchip lasers was investigated. Laser pulses at 1030 nm with pulse width of 466 ps and peak power of 91 kW were achieved with cavity length of 1.7 mm, while laser pulses with pulse width of 665 ps and peak power of 79 kW were obtained with cavity length of 3.7 mm.

1. Introduction

Owing to their compactness, cavity-alignment-free, high beam quality, Cr^{4+}:YAG passively Q-switched microchip lasers with high peak power are widely used in laser processing, laser ignition, efficient nonlinear frequency conversion and so on [1,2]. Composite crystals have been widely used in constructing compact passively Q-switched miniature lasers by bonding Nd:YAG crystal and Cr^{4+}:YAG crystal together. Recently, Nd:YAG/Cr^{4+}:YAG composite ceramic passively Q-switched microchip lasers pumped by quasi-continuous-wave (QCW) laser-diode have been demonstrated with MW peak power [3,4]. However, the optical–optical conversion efficiency of Nd:YAG/Cr^{4+}:YAG composite ceramic passively Q-switched lasers was less than 19%. The highest optical-to-optical efficiency of 29% was achieved from a Nd:YAG/Cr:YAG composite crystal passively Q-switched laser [5]. Compared to Nd:YAG laser crystal, Yb:YAG crystal is more favorite for developing passively Q-switched microchip lasers because it has small quantum defect (8.6%) for efficient laser operation, small emission cross section for obtaining high pulse energy, long lifetime for energy storage [6], and high doping concentration for microchip lasers [7]. High peak power Yb:YAG/Cr^{4+}:YAG composite ceramic passively Q-switched microchip lasers has been demonstrated with peak power of 0.72 MW [8]. Passively Q-switched diffusion bonded Yb:YAG/Cr:YAG microchip laser with a volume Bragg grating (VBG) mirror has been cidemonstrated with optical efficiency of 26% and a very low pulse timing jitter [9]. Yb:YAG/Cr^{4+}:YAG composite crystal lasers have been demonstrated with external and microchip resonators, however, the optical breakdown occurred in the surfaces of Yb:YAG/Cr^{4+}:YAG composite crystal for microchip cavity, and the optical efficiency was less than 5% in external cavity [10]. Quasi-CW laser-diode pumped Cr^{4+}:YAG passively Q-switched Yb:YAG micro-laser has been demonstrated with optical efficiency of 25% [11]. The thermal loading of Yb:YAG crystal limits the laser efficiency. And the quasi-three-level property of Yb:YAG crystal causes the population in lower laser level to increase significantly with rising temperature of Yb:YAG crystal induced by the pump power. Enhanced performance of Cr^{4+}:YAG passively Q-switched Yb:YAG laser with diamond surface cooling has been demonstrated with optical efficiency of 25% [12]. Efficient performance of passively Q-switched Yb:YAG/Cr,Yb:YAG and Yb:YAG/Cr^{4+}:YAG lasers with efficiencies of 32% and 44% have been demonstrated with high-brightness single-emitter laser-diode pumping [13,14]. However, the pulse energy was limited by the high initial transmission of saturable absorber.

In this paper, microchip laser performance of Yb:YAG/Cr^{4+}:YAG composite crystal fabricated with thermal bonding technology has been studied. Highly efficient passively Q-switch microchip laser of Yb:YAG/Cr^{4+}:YAG composite crystal has been demonstrated under high-brightness laser-diode pumping. The highest optical-to-optical efficiency of over 41% has been achieved in

* Corresponding author. Tel.: +86 5922580004.
E-mail address: jdong@xmu.edu.cn (J. Dong).

0030-4018/$ - see front matter
http://dx.doi.org/10.1016/j.optcom.2013.09.030

Yb:YAG/Cr^{4+}:YAG composite crystal, to our best knowledge. The average output power of 1.5 W was obtained. The effect of the cavity lengths on microchip laser performance was studied and the short laser pulse width was achieved in passively Q-switched Yb:YAG/Cr^{4+}:YAG lasers with short laser cavity. Laser pulses with pulse energy of 43 μJ, pulse width of 466 ps, peak power of over 91 kW were obtained.

2. Experimental setup

The experimental setup of laser-diode pumped Yb:YAG/Cr^{4+}:YAG composite crystal passively Q-switched microchip lasers is similar to those used in Yb:YAG/Cr,Yb:YAG and Yb:YAG/Cr^{4+}:YAG microchip laser [13,14]. The Yb:YAG/Cr^{4+}:YAG composite crystal fabricated with thermal bonding technology was used in the laser experiments. Based on our previous experimental results and theoretical modeling of Yb:YAG microchip lasers [15,16] and Cr^{4+}:YAG passively Q-switched Yb:YAG microchip lasers [17–19], the thicknesses of Yb:YAG part and Cr^{4+}:YAG part in Yb:YAG/Cr^{4+}:YAG composite crystal are set to 1.2 mm and 0.5 mm, respectively, and the total thickness of Yb:YAG/Cr^{4+}:YAG composite crystal is 1.7 mm. The doping concentration of Yb^{3+} ions is 10 at.% and the initial transmission of Cr^{4+}:YAG is 90%. The Yb:YAG surface is coated with anti-reflection at 940 nm and highly reflection at 1030 nm to act as rear cavity mirror of the laser. The Cr^{4+}:YAG surface was uncoated. Based on our previous works of Yb:YAG/Cr,Yb:YAG microchip laser and separated Yb:YAG, Cr^{4+}:YAG microchip laser [13,14], the plane-parallel cavity mirror with 50% transmission was chosen as output coupler to avoid coating damage under high peak power laser operation. The composite Yb:YAG/Cr^{4+}:YAG crystal and output coupling mirror are mounted in the middle of two copper blocks with a 5 mm-diameter hole in the center. The cavity lengths of 1.7 mm and 3.7 mm were set for investigating the laser performance of Yb:YAG/Cr^{4+}:YAG composite crystal. A high-brightness single-emitter laser-diode with a 1 μm × 50 μm emitting cross section was used as the pump source. The fast-axis divergence angle of the laser-diode was shaped to 10° with a micro-lens at the output facet of laser-diode. Two lenses with 11 mm focal length were used to collimate and focus the pump beam on the Yb:YAG crystal rear surface. The footprint of the focus spot was measured to be 80 × 80 μm^2. The laser experiment was carried out at room temperature without active cooling system. The average output power was measured with a Thorlabs PM200 power meter. The laser emitting spectra of the lasers were measured with an Anritus optical spectral analyzer (MS9740A). The laser pulse characteristics were detected with a 5 GHz InGaAs photo-diode and recorded with a 6 GHz bandwidth Tektronix digital phosphor oscilloscope (TDS6604).

3. Results and discussion

The absorbed pump power of Yb:YAG/Cr^{4+}:YAG composite crystal was obtained by measuring the incident pump power after optical coupling system and residual power after Yb:YAG/Cr^{4+}:YAG composite crystal under no lasing condition. The pump power absorption efficiency of Yb:YAG/Cr^{4+}:YAG composite crystal was measured to be 60%. The low absorption efficiency of Yb:YAG/Cr^{4+}:YAG composite crystal was attributed to the mismatch of the pump wavelength and the peak absorption wavelength of Yb:YAG crystal. The average output power and the optical-to-optical efficiency (η_{O-O}) of Yb:YAG/Cr^{4+}:YAG composite crystal passively Q-switched microchip lasers as a function of the absorbed pump power were shown in Fig. 1. For microchip laser with 1.7 mm cavity length, the absorbed pump power threshold was 0.32 W. The average output power increases linearly with the absorbed pump power when the absorbed pump power was less than 2 W. The slope efficiency was measured to be 45.5%. The average output power tended to increase slowly when the absorbed pump power was higher than 2 W. The maximum optical-to-optical efficiency of 37% was obtained when the absorbed pump power was 2 W. When the cavity length was set to 3.7 mm, the absorbed pump power threshold was increased to 0.5 W. The average output power increased linearly with the absorbed pump power and no output power saturation was observed. The slope efficiency was measured to be 52.3%. The maximum average output power of 1.5 W was obtained at the absorbed pump power of 3.65 W, the corresponding optical-to-optical efficiency of 41% was achieved, which was 1.6 times of that obtained with a diamond surface cooling [12], 11 times of that obtained Yb:YAG/Cr^{4+}:YAG composite crystal long cavity lasers [10] and at least 40% higher than that of Nd:YAG/Cr:YAG laser [5]. The highly efficient laser performance of Yb:YAG/Cr^{4+}:YAG composite crystal was attributed to the high pump power intensity, and good mode overlap between laser and pump beam. The pump power intensity applied on Yb:YAG/Cr^{4+}:YAG composite crystal passively Q-switched microchip laser reaches up to about 94 kW/cm^2 at the incident pump power of 6 W. Such high pumping intensity depletes the ground state population of Yb:YAG crystal and increases the inversion population for efficient laser operation. Depletion of the ground state population alleviates the thermal effect of Yb:YAG crystal, then improves the laser performance.

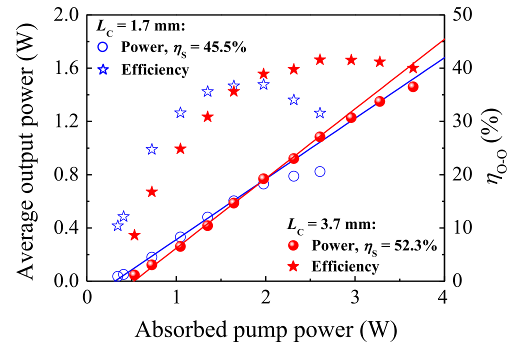

Fig. 1. Average output power and optical-to-optical efficiency of Yb:YAG/Cr^{4+}:YAG composite crystal passively Q-switched microchip lasers as a function of the absorbed pump power for different cavity lengths. Lines are the linear fits of experimental data.

The stable oscillation of Yb:YAG/Cr^{4+}:YAG composite crystal passively Q-switched microchip lasers was attributed to the thermal lens effect although the thermal effect degrades the laser performance. The thermal focal length, f, of Yb:YAG/Cr^{4+}:YAG composite crystal passively Q-switched microchip lasers can be expressed as [20]

$$f = \frac{\pi K_c w_p^2}{P_h (dn/dT)} \frac{1}{1-\exp(-\alpha l)} \quad (1)$$

where w_p is the radius of pump beam, K_c is the thermal conductivity, dn/dT is the change in refractive index with temperature, P_h is the heat generated inside the gain medium, α is the absorption coefficient of Yb:YAG crystal, and l is the length of Yb:YAG crystal. Consequently, the focus length f decreases with temperature. Under the absorbed pump power of 2.61 W, the focal length f of Yb:YAG/Cr:YAG is 13 mm. For microchip laser resonator with an internal thermal focal lens introduced by the thermal effect, when the end face deformation of gain medium is neglected, the mode spot size at one cavity mirror can be expressed as a function of the resonator

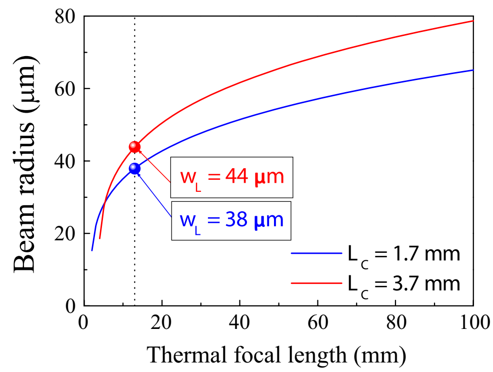

Fig. 2. The calculated laser mode radius at output coupler of Yb:YAG/Cr^{4+}:YAG composite crystal passively Q-switched microchip lasers as a function of the thermal lens focal length for different cavity lengths. The dots show the mode radii for thermal lens focal length of 13 mm at the absorbed pump power of 2.61 W.

parameters as follows [21],

$$w_1^2 = \frac{\lambda L}{\pi}\left(\frac{g_2}{g_1(1-g_1 g_2)}\right)^{1/2} \tag{2}$$

$$w_2^2 = \frac{g_1}{g_2} w_1^2 \tag{3}$$

where $g_1 = 1 - L_2/f - L_0/R_1$, $g_2 = 1 - L_1/f - L_0/R_2$, $L_0 = L_1 + L_2 - (L_1 L_2/f)$, and f is the focal length of the internal lens; L_1 and L_2 are the spacings between cavity mirrors and the lens, R_1 and R_2 are the curvature of the two cavity mirrors, $R_1 = R_2 = \infty$ for microchip laser cavity.

Taking into account the temperature dependent thermal conductivity, thermal expansion coefficient, the change of the refractive index with temperature of Yb:YAG crystal [22], the mode spot radius on the output mirror as a function of the thermal lens focal length for $L_C = 1.7$ mm and $L_C = 3.7$ mm is shown in Fig. 2. The laser mode spot radii of Yb:YAG/Cr^{4+}:YAG composite crystal passively Q-switched microchip lasers increase with thermal lens focal length for different cavity lengths. The longer the cavity length, the larger the laser modes obtained under the same thermal lens focal length. The mode spot radii of the Yb:YAG/Cr^{4+}:YAG composite crystal passively Q-switched lasers were calculated to be 38 μm and 44 μm for $L_C = 1.7$ mm and $L_C = 3.7$ mm, respectively, when the pump beam radius of 45 μm and absorbed pump power of 2.61 W were used. Therefore, the laser beam area for $L_C = 3.7$ mm is about 1.34 times of that for $L_C = 1.7$ mm. The pulse energy of passively Q-switched microchip laser is proportional to the laser mode area, the pulse energy for $L_C = 3.7$ mm is larger than that for $L_C = 1.7$ mm. The repetition rate nearly keeps the same for two different cavity lengths since the repetition rate is governed by the inversion population provided by the pump power. Thus, the average output power for $L_C = 3.7$ mm is higher than that for $L_C = 1.7$ mm under the same pump power levels.

The measured laser emitting spectra show that the Yb:YAG/Cr^{4+}:YAG composite crystal passively Q-switched microchip lasers oscillate in multi-longitudinal-mode for two cavity lengths. The number of longitudinal modes increases with the absorbed pump power. Fig. 3 shows the laser emitting spectra of Yb:YAG/Cr^{4+}:YAG passively Q-switched microchip lasers at different absorbed pump power levels for two cavity lengths. Two longitudinal modes oscillate for $L_C = 1.7$ mm while three longitudinal modes oscillate for $L_C = 3.7$ mm when the absorbed pump power is 1.05 W, as shown in Fig. 3(a), and the oscillating wavelength for $L_C = 1.7$ mm is shorter than that for $L_C = 3.7$ mm. The laser oscillates at two longitudinal modes for $L_C = 1.7$ mm and five longitudinal modes for $L_C = 3.7$ mm at the absorbed pump power of 1.64 W, respectively.

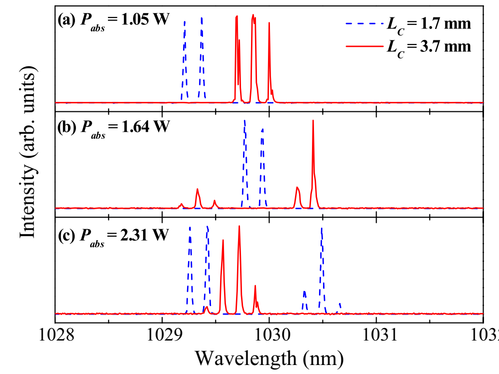

Fig. 3. The laser emitting spectra of Yb:YAG/Cr^{4+}:YAG composite crystal passively Q-switched microchip lasers under different pump power levels for two different cavity lengths.

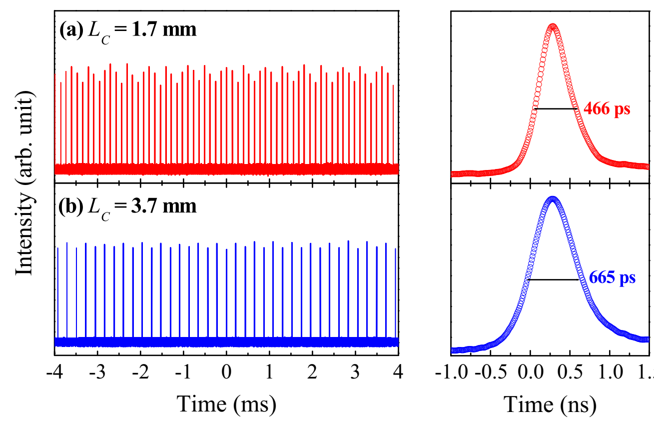

Fig. 4. Typical pulse trains and pulse profiles of Yb:YAG/Cr^{4+}:YAG composite crystal passively Q-switched microchip lasers.

Further increase pump power, the laser oscillates at five longitudinal modes for $L_C = 1.7$ mm and four longitudinal modes for $L_C = 3.7$ mm at the absorbed pump power of 2.31 W. The mode separation between longitudinal modes were measured to be 0.16 nm and 0.15 nm for $L_C = 1.7$ mm and $L_C = 3.7$ mm, respectively. The free spectral range is 0.17 nm and 0.086 nm for $L_C = 1.7$ mm and $L_C = 3.7$ mm, respectively. The mode separation for $L_C = 1.7$ mm is in good agreement with the free spectral range, while the mode separation for $L_C = 3.7$ mm is two times of the free spectra range, which is determined by the mode selection of 1.7 mm-thick Yb:YAG/Cr^{4+}:YAG composite crystal plate. At high pump power levels, the wide separation of longitudinal modes was attributed to the strong mode competition.

Fig.4 shows the typical pulse trains and laser pulse profiles of Yb:YAG/Cr^{4+}:YAG composite crystal passively Q-switched microchip lasers at the absorbed pump power of 1.05 W for two different cavity lengths. The laser pulse train exhibits periodical pulsation for $L_C = 1.7$ mm, as shown in Fig. 4(a). The corresponding pulse profile with pulse width of 466 ps and peak power of 91 kW was observed. The laser pulse train exhibits stable pulsation for $L_C = 3.7$ mm, as shown in Fig. 4(b), the corresponding laser pulse with pulse width of 665 ps and peak power of 79 kW was achieved. The multi-longitudinal mode oscillation of Yb:YAG/Cr^{4+}:YAG composite crystal passively Q-switched microchip lasers was attributed to the periodical pulsation [23]. It should be noted that any individual laser pulse oscillated on a single-longitudinal mode. However, owing to the gain and loss are different for different longitudinal modes for Yb:YAG/Cr^{4+}:YAG passively Q-switched microchip lasers, the laser pulse energy for any

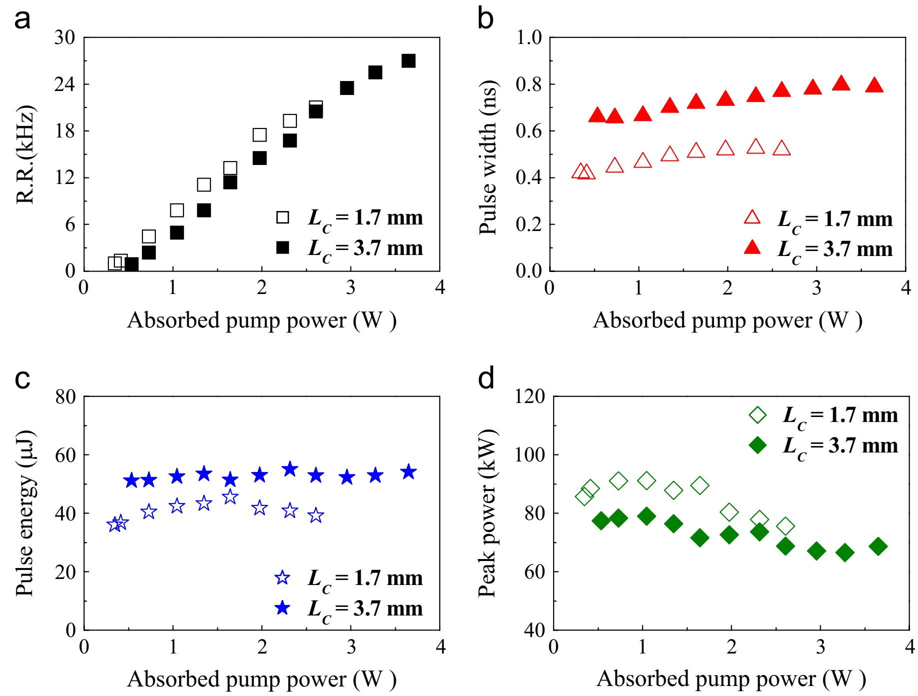

Fig. 5. Repetition rate, pulse width, pulse energy and peak power of Yb:YAG/Cr^{4+}:YAG composite crystal passively Q-switched microchip lasers as a function of the absorbed pump power.

individual laser pulse are different in intensities, therefore, the total laser pulse train of passively Q-switched Yb:YAG microchip laser exhibits periodical pulsation.

Fig.5 shows the variation of repetition rate, pulse width, pulse energy and peak power of Yb:YAG/Cr^{4+}:YAG composite crystal passively Q-switched microchip lasers with the absorbed pump power for two different cavity lengths. The repetition rate increases nearly linearly with the absorbed pump power for two different cavity lengths. For L_C=1.7 mm, the repetition frequency increases linearly to 17.5 kHz with the absorbed pump power and the increase ratio is 10.5 kHz/W. For L_C=3.7 mm, the repetition rate increases linearly to 27 kHz with the absorbed pump power. The increase ratio of the repetition rate is 9 kHz/W. Under the same pump power levels, the repetition rate for L_C=1.7 mm is higher than that for L_C=3.7 mm. The pulse width increases from 420 ps to 520 ps with the absorbed pump power for L_C=1.7 mm, the pulse width increases from 660 ps to 790 ps with the absorbed pump power for L_C=3.7 mm. The pulse width for L_C=3.7 mm is about 50% wider than that for L_C=1.7 mm at the same absorbed pump power, which is caused by the long cavity length. The broadening of the pulse width with the absorbed pump power is attributed to the thermal effect under the high pump power intensity. The initial transmission of Cr^{4+}:YAG crystal increases with the temperature [24], while the pulse width is governed by the initial transmission of the saturable absorber, the higher the initial transmission of the saturable absorber, the wider the output pulse. The pulse energy increases slowly with the absorbed pump power when the absorbed pump power is lower than 1.65 W and then tends to decrease with the absorbed pump power for L_C=1.7 mm. The pulse energy nearly keeps constant with the absorbed pump power for L_C=3.7 mm. The highest pulse energy of 54 μJ was obtained for L_C=3.7 mm, which was about 30% higher than that obtained for L_C=1.7 mm. This is attributed to the large laser mode of longer cavity, the laser beam area for L_C=3.7 mm is about 1.34 time of that for L_C=1.7 mm, therefore, high energy was achieved for L_C=3.7 mm. The peak power nearly keeps constant and then tends to decrease slightly with the absorbed pump power for L_C=1.7 mm, while the peak power decreases slowly and then tends to keep constant with the absorbed pump power for L_C=3.7 mm. This was caused by the pulse broadening with the absorbed pump power. The highest peak power of 91 kW was achieved for L_C=1.7 mm, which was about 1.15 of that for L_C=3.7 mm. The high peak power Yb:YAG/Cr^{4+}:YAG composite crystal passively Q-switched microchip lasers could be achieved by adopting large pump beam area under high pump power intensity, while the optical efficiency can be maintained by adjusting the cavity lengths with bonging undopded YAG to Yb:YAG/Cr^{4+}:YAG composite crystal.

Theoretical models of passively Q-switched lasers have been successfully used to simulate and predict the laser performance of passively Q-switched quasi-three-level lasers [25–28]. With the aid of the theoretical model that was successfully applied to the early Yb:YAG/Cr^{4+}:YAG composite ceramic laser [19], numerical calculations of laser performance of Yb:YAG/Cr^{4+}:YAG composite crystal were carried out under the current experimental conditions. The values of the parameters involved in these calculations are listed, adopting the same symbols as in the model [17,19], as follows: $\sigma_g=4.3\times10^{-18}$ cm^2 and $\sigma_e=8.2\times10^{-19}$ cm^2 for Cr^{4+}:YAG; $\sigma=2.3\times10^{-20}$ cm^2 and τ=951 μs for Yb:YAG; L=0.01; w_p=45 μm; w_L=38 μm and 44 μm for L_C=1.7 mm and L_C=3.7 mm, respectively. The incident pump power of 4.5 W was used in the numerical calculations. The calculated pulse energy, pulse width, peak power and repetition rate, 51 μJ, 442 ps, 116 kW and 21.6 kHz for L_C=1.7 mm; and 56 μJ, 747 ps, 75 kW and 21.5 kHz for L_C=3.7 mm, are in fairly good agreement with the experimental results when the absorbed pump power of 2.61 W was applied.

4. Conclusion

Highly efficient laser performance of Yb:YAG/Cr^{4+}:YAG composite crystal has been demonstrated by adopting high pump power intensity. Average output power of 1.5 W was achieved at the absorbed pump power of 3.65 W. The optical-to-optical efficiency of 41% and slop efficiency of 52.3% were achieved in laser-diode pumped Yb:YAG/Cr^{4+}:YAG composite crystal passively Q-switched microchip lasers. The cavity lengths have great effects on the laser performance of Yb:YAG/Cr^{4+}:YAG composite crystal. The laser pulses with pulse energy of 43 μJ, pulse width of 466 ps and peak power of 91 kW were obtained for L_C=1.7 mm, while lasers pulse with pulse energy of 54 μJ, pulse width of 665 ps and peak power of 79 kW was obtained for L_C=3.7 mm. Although high pulse energy was obtained with long cavity length, the high peak power was generated in short cavity microchip laser owing to the short pulse generation.

Acknowledgment

This work was supported by a Grant from the National Natural Science Foundation of China (61275143), the Program for New Century Excellent Talents in University (NCET-09–0669), the Fundamental Research Funds for the Central Universities (2010121058), the Ph.D. Programs Foundation of Ministry of Education of China (20100121120019).

References

[1] H. Kofler, J. Tauer, G. Tartar, K. Iskra, J. Klausner, G. Herdin, E. Wintner, Laser Physics Letters 4 (2007) 322.
[2] T. Taira, Optical Materials Express 1 (2011) 1040.
[3] N. Pavel, M. Tsunekane, T. Taira, Optics Express 19 (2011) 9378.
[4] O. Sandu, G. Salamu, N. Pavel, T. Dascalu, D. Chuchumishev, A. Gaydardzhiev, I. Buchvarov, Quantum Electronics 42 (2012) 211.
[5] Y. Kalisky, L. Kravchik, M.R. Kokta, Optical Materials 24 (2004) 607.
[6] Y. Kalisky, C. Labbe, K. Waichman, L. Kravchik, U. Rachum, P. Deng, J. Xu, J. Dong, W. Chen, Optical Materials 19 (2002) 403.
[7] F.D. Patel, E.C. Honea, J. Speth, S.A. Payne, R. Hutcheson, R. Equall, IEEE Journal of Quantum Electronics 37 (2001) 135.
[8] J. Dong, K. Ueda, A. Shirakawa, H. Yagi, T. Yanagitani, A.A. Kaminskii, Optics Express 15 (2007) 14516.
[9] C. Sotelo, R.D. Stultz, Advanced Solid-State Photonics, Optical Society of America, San Diego, CA (2012) AT4A.12.
[10] J. Sulc, T. Koutny, H. Jelinkova, K. Nejezchleb, V. Skoda, Solid State Lasers XXI: Technology and Devices, in: W.A. Clarkson, R.K. Shori (Eds.), Proceedings of SPIE, 8235, 2012, p. 823522.
[11] M. Tsunekane, T. Taira, Proceedings of the Conference on Lasers and Electro-Optics, Optical Society of America, San Jose, California, 2012, p. JW2A.27.
[12] W.Z. Zhuang, Y.F. Chen, K.W. Su, K.F. Huang, Y.F. Chen, Optics Express 20 (2012) 22602.
[13] Y. Cheng, J. Dong, Y.Y. Ren, Optics Express 20 (2012) 24803.
[14] J. Dong, G.Y. Wang, Y. Cheng, Laser Physics 23 (2013) 035802.
[15] J. Dong, A. Shirakawa, K.I. Ueda, A.A. Kaminskii, Applied Physics B: Lasers and Optics 89 (2007) 359.
[16] J. Dong, A. Shirakawa, K.I. Ueda, A.A. Kaminskii, Applied Physics B: Lasers and Optics 89 (2007) 367.
[17] J. Dong, Optics Communications 226 (2003) 337.
[18] J. Dong, A. Shirakawa, K.I. Ueda, Applied Physics B: Lasers and Optics 85 (2006) 513.
[19] J. Ma, J. Dong, K. Ueda, A.A. Kaminskii, Applied Physics B: Lasers and Optics 105 (2011) 749.
[20] M.E. Innocenzi, H.T. Yura, C.L. Fincher, R.A. Fields, Applied Physics Letters 56 (1990) 1831.
[21] W. Koechner, Solid State Laser Engineering, Springer-Verlag, Berlin, 1999.
[22] R. Wynne, J.L. Daneu, T.Y. Fan, Applied Optics 38 (1999) 3282.
[23] J. Dong, A. Shirakawa, K. Ueda, Laser Physics Letters 4 (2007) 109.
[24] M. Tsunekane, T. Taira, Proceedings of the Conference on Lasers and Electro-Optics/International Quantum Electronics Conference, Optical Society of America, Baltimore, Maryland, 2009, p. JTuD8.
[25] J.J. Degnan, IEEE Journal of Quantum Electronics, 31 (1995) 1890.
[26] G.H. Xiao, M. Bass, IEEE Journal of Quantum Electronics 33 (1997) 41.
[27] X.Y. Zhang, S.Z. Zhao, Q.P. Wang, Q.D. Zhang, L.K. Sun, S.J. Zhang, IEEE Journal of Quantum Electronics 33 (1997) 2286.
[28] F.D. Patel, R.J. Beach, IEEE Journal of Quantum Electronics 37 (2001) 707.